



**University of
Zurich**^{UZH}

**Zurich Open Repository and
Archive**

University of Zurich
University Library
Strickhofstrasse 39
CH-8057 Zurich
www.zora.uzh.ch

Year: 2019

Characterization of the optical properties of color pastes for the design of optical phantoms mimicking biological tissue

Tomm, Natasha ; Ahnen, Linda ; Isler, Helene ; Kleiser, Stefan ; Karen, Tanja ; Ostojic, Daniel ; Wolf, Martin ; Scholkmann, Felix

Abstract: Clinicians need a way to rapidly and reliably test the correct functioning of near-infrared spectroscopy (NIRS)-based oximeters. Therefore, optical phantoms for quality assessment of NIRS oximeters are needed. The fabrication of such phantoms that mimic the optical properties of biological tissue in the NIR range represents a challenge. To enable their development, the aim was to characterize the absorption and scattering spectra of different dyes. The optical properties of silicone SILPURAN 2420 with 11 color pastes of type ELASTOSIL were measured in the 500 to 1000 nm range by a spectrometer with an integrating sphere. In addition, two commercial frequency-domain NIRS devices, the ISS OxiplexTS and the ISS Imagent, were used to assess the optical properties at specific wavelengths. The evaluated colors present mostly features in the visible range below 650 nm, but two colors include peaks in the near-infrared region, simulating low tissue oxygenation values. These colors were used to create an optical phantom, which matched the designed StO value within an error of only 4%. This set of dyes already enables simulating many different spectra, thus achieving a first step on the way to a long-term stable comparison and validation method.

DOI: <https://doi.org/10.1002/jbio.201800300>

Posted at the Zurich Open Repository and Archive, University of Zurich

ZORA URL: <https://doi.org/10.5167/uzh-161769>

Journal Article

Accepted Version

Originally published at:

Tomm, Natasha; Ahnen, Linda; Isler, Helene; Kleiser, Stefan; Karen, Tanja; Ostojic, Daniel; Wolf, Martin; Scholkmann, Felix (2019). Characterization of the optical properties of color pastes for the design of optical phantoms mimicking biological tissue. *Journal of Biophotonics*, 12(4):e201800300.

DOI: <https://doi.org/10.1002/jbio.201800300>

Article type: Full Article

Characterization of the optical properties of color pastes for the design of optical phantoms mimicking biological tissue

Natasha Tomm^{1,}, Linda Ahnen¹, Helene Isler^{1,*}, Stefan Kleiser¹, Tanja Karen¹, Daniel Ostojic¹, Martin Wolf¹ and Felix Scholkmann¹*

*Corresponding Authors: E-mails: natasha.tomm@unibas.ch, helene.isler@usz.ch

¹Biomedical Optics Research Laboratory, Department of Neonatology, University Hospital Zurich, 8091 Zurich, Switzerland

Keywords: near-infrared spectroscopy (NIRS), inverse adding-doubling (IAD), UV/VIS spectroscopy, optical phantoms, oximetry

Short title: N. Tomm et al.: Characterization of dyes for specific design of optical phantoms

Clinicians need a way to rapidly and reliably test the correct functioning of near-infrared spectroscopy (NIRS) based oximeters. Therefore, optical phantoms for quality assessment of NIRS oximeters are needed. The fabrication of such phantoms that mimic the optical properties of biological tissue in the NIR range represents a challenge. To enable their development, the aim was to characterize the absorption and scattering spectra of different dyes. The optical properties of silicone SILPURAN® 2420 with 11 color pastes of type ELASTOSIL® were measured in the 500–1000 nm range by a spectrometer with an integrating sphere. In addition, two commercial frequency-domain NIRS devices, the ISS OxiplexTS™ and the ISS Imagent™ were employed to assess the optical properties at specific wavelengths. The evaluated colors present mostly features in the visible range below 650 nm, but two colors include peaks in the near-infrared region, simulating low tissue oxygenation values. These colors were employed to create an optical phantom, which matched the designed StO₂ value within an error of only 4%. This set of dyes already enables simulating many different spectra, thus achieving a first step on the way to a long-term stable comparison and validation method.

1. Introduction

Near-infrared spectroscopy (NIRS) based oximeters are able to non-invasively monitor absolute values of tissue oxygen saturation (StO_2) and hemodynamics in real-time at the bedside. Abnormal such parameters may reflect dangerous situations that could lead to lesions and thus enable to guide clinical treatment to prevent morbidities.[1-3] Most instruments employ disposable inexpensive low-quality sensors, which break from time to time. Thus, if such an instrument displays abnormal values while a patient seems to be fine, clinicians need a method to test accurate functioning. Such a test needs to be fast and simple.

So far, in-vivo studies [4, 5] and studies in liquid phantoms,[6-8] made from IntralipidTM and human hemoglobin were performed and shown to be appropriate for evaluating NIRS systems.[7] These studies are, however, generally time consuming, work intensive and cannot serve as a quick quality control. As a solution, we propose to build stable and easily disinfectable solid phantoms. These can be designed to mimick properties of biological chromophores, in particular oxy- and deoxyhemoglobin, over a wide spectral range to be valid for various NIRS instruments. However, the creation of a realistic absorption spectrum is not trivial. It may be achieved by incorporating blood into solid phantoms,[9] but such phantoms are only stable for up to four months. Thus, our approach is to perform a mixture of different chromophores whose combined absorption in specific regions of interest may represent oxy- and deoxyhemoglobin. In addition, such phantoms will have favorable properties such as ease of fabrication, storage, transportation, reproducibility and low cost. Nevertheless, producing such a phantom requires designing its absorption and scattering properties not only at specific wavelengths, but also over a certain wavelength range. This has not been achieved yet. The aim therefore was to characterize the optical properties of different dyes that can selectively be incorporated in solid phantoms to design a specific absorption spectrum.

2. Theoretical Background

The absorption coefficient μ_a of a material is given by the sum of the individual molar extinction coefficient ε_i of each chromophore multiplied by their molar concentrations c_i ,

$$\mu_a(\lambda) = \ln(10) \sum_{i=1}^N c_i \cdot \varepsilon_i(\lambda), \quad (1)$$

where N is the number of chromophores. Similarly, the reduced scattering coefficient (μ_s') is proportional to the concentration of scatterers.[10]

To design a specific absorption spectrum \vec{M} for an ensemble of k wavelengths $\lambda_1, \lambda_2, \dots, \lambda_k$, the concentrations of chromophores \vec{C} are given by the non-negative solutions of the minimization problem posed by

$$\min_c \frac{1}{2} \left\| \ln(10) E \cdot \vec{C} - \vec{M} \right\|^2, \text{ s.t. } C_i \geq 0. \quad (2)$$

E is a $k \times N$ matrix representing the molar extinction coefficients of the different chromophores. Concentrations C_i cannot be negative. Thus, different spectra of absorption and scattering of an optical phantom may be designed according to Eq. (2) by combining dyes with known optical absorption properties.

3. Methods

The μ_a and μ_s' of 11 biocompatible silicone-soluble color pastes of type ELASTOSIL® (*Wacker Chemie AG*, Munich, Germany) were investigated: Yellow RAL 1016, Orange RAL 2004, Red Violet RAL 4002, Dark Blue RAL 5010, Helio Green RAL 6004, Green RAL 6010, Black RAL 9011, Blue RAL 5022, Dark Red RAL 3000, White RAL 9010, Yellow RAL 1026. The batch numbers of these color pastes are specified in the Appendix S1, **Table A1**.

To determine the optical properties for each color paste, 9 thin silicone phantoms were fabricated with 3 different dye concentrations at 3 thicknesses. These met the requirements of homogeneity, thickness, surface smoothness and sample diameter for evaluation with an

integrating sphere [11-13] and the Inverse Adding-Doubling (IAD) software.[14, 15] To create long-lasting and low-cost phantoms, the biocompatible silicone SILPURAN® 2420 A/B (Wacker Chemie AG, Munich, Germany) with a weight mix ratio of components A and B of 1:1 has been used as the base material. For each of the 11 colors, 2 g of paste were diluted in 200 ml component A. This primary mixture will be called *dye dilution* in the following. Since it is difficult to extract a precise amount of paste due to the trace amounts needed, taking this dye dilution minimizes the mixing error in the exact color paste concentration in the phantom. To estimate errors, for each paste 3 different concentrations of dye dilution c_{dye}^j ($j = 1, 2, 3$), being $c_{\text{dye}}^1=5.0$ ml, $c_{\text{dye}}^2=2.5$ ml, $c_{\text{dye}}^3=0.5$ ml, were thoroughly mixed with a complementary volume of component A, such that the sum of the volume of component A and dye dilution was always 20.0 ml. Finally, 20.0 ml of component B were added and thoroughly mixed until homogeneity was reached. To avoid bubbles when cured, the mixture was degassed with a vacuum pump.

For each phantom batch, thin samples of 1.0 mm, 1.5 mm and 2.0 mm thickness were cast using C-mount Spacer Rings (ThorLabs®, Dachau/Munich, Germany) as casting molds. The choice of thicknesses was based on the requirement for accurate analysis using IAD,[12] i.e. that the sample thickness should be $\sim 1/10$ of the port diameter of the spectrometer. The rings had entry holes carved on the side and were compressed between plastic blocks, held by pressure clamps. As IAD assumes the samples to have a smooth non-specular surface,[12] the plastic blocks were wet-sanded with FEPA-graded sandpapers P340, P600 and P800 successively, until no scratches were visible.[16] Any residuals of the sanding process were removed by pouring a thin layer of silicone onto the plastic block, letting it cure and peeling it off. Finally, the phantom mixture was injected into the casting mold with syringes (Appendix S1, **Figure A1**) and placed in the oven at 80 °C to accelerate the curing process.

After 60 minutes, the plastic blocks were separated, the phantoms peeled off the casting mold and any excess material trimmed. An example of thin phantoms is shown in **Figure 1**.

3.1. Determination of the Absorption Spectra

The total transmittance T , total reflectance R and unscattered transmittance U were measured between 500 nm and 1000 nm in 1 nm intervals for each of the 9 thin phantoms of each color.

The measurements were performed with the Spectrometer Shimadzu UV 1610 (*Shimadzu Corporation*, Kyoto, Japan) employing the standard measurement layout for the

U measurement mode. T and R measurements were performed with an integrating sphere according to IAD's manual.[14] Every measurement was conducted three times (delivering $M_k^{\text{sample } j}$ with $j \in \{1, 2, \dots, 9\}$, $k \in \{1, 2, 3\}$, $M \in \{T, R, U\}$). As expected, most of the repeated measurement spectra were well reproduced, i.e. the spectra of these measurements overlap. A few spectra with deformations and offsets were eliminated by considering only the *median dataset* of the three spectra for further analysis.[17]

The μ_a spectrum of each sample was determined by an adapted point-to-point analysis with the IAD software. The IAD routine was applied twice to each median dataset $(\bar{U}, \bar{R}, \bar{T})^{\text{phantom } j}$. In the first run, initial spectra of μ_a and μ_s' , as well as of the anisotropy factor g , were determined with standard IAD analysis. At high peaks in the absorption curves, anomalous behavior in the μ_s' curves were observed. Subsequently, a corrected μ_s' curve was calculated by fitting a decaying-exponential curve to the normal parts of the original μ_s' curve and extrapolating to the whole interval (500 nm – 1000 nm). This correction, applied in the second run, is justified by the Mie approximation $\mu_s'(\lambda) = \alpha \cdot \lambda^{-\beta}$, where α and β are constants to be determined for each case.[18] Noticing that most of the dyes presented forward scattering with $g \sim 0.9$, this value was chosen as the standard factor in the second run, the adapted point-to-point analysis. Fixing the values of μ_s' and g to the corrected values at each wavelength, and providing again the measured $(\bar{U}, \bar{T}, \bar{R})^{\text{phantom } j}$, IAD was able to

return reliable values over the entire spectral range. This method of analysis using two runs influences only the anomalous regions of the spectrum and was, therefore, applied for all phantom spectra.

For each concentration of dye dilution, the μ_a curves of the three thicknesses should overlap, indicating that the analysis was correct. In summary, for 11 colors we manufactured 9 thin phantoms (3 thicknesses \times 3 concentrations) and measured each phantom three times. For each repetitive measurement and thickness, we determined a spectrum and the resulting median dataset was employed in the further analysis working with three μ_a spectra per color.

3.2. Inherent Reduced Scattering Coefficient

When calculating the μ_s' of the thin phantoms with IAD, all color pastes, except White RAL 9010, presented similar μ_s' values (between 0.2 mm^{-1} and 0.4 mm^{-1}) even for different concentrations of dye dilution. Furthermore, while the μ_s' should remain constant for the same concentration, we observed higher μ_s' for thinner samples.

To further investigate this behavior on color Blue RAL 5010, three 600 ml silicone phantoms were cast, as described in Sec. 3, in molds of $9.6 \times 7.0 \times 10.6 \text{ cm}^3$, with different concentrations. Thin phantoms, for the IAD analysis, of the same batches were also fabricated and evaluated as described in Subsec. 3.1. This enabled a direct comparison between frequency domain NIRS and spectrophotometric measurements of the same silicone mixture. These phantoms had a basic mixture, which in the following will be called *scattering dilution*. It consisted of 600 μl of the color White RAL 9010 and 164 μl of a dilution produced with carbon black powder (Alpha Aesar, Thermo Fisher GmbH, Karlsruhe, Germany) into silicone component A, which will be referred to as carbon black stock dilution in the following. The recipe for each phantom is shown in **Table 1**. Thus, scattering originating from Blue RAL 5022 and White RAL 9010 was evaluated and differentiated. It was already known that carbon black does not contribute to μ_s' and has an approximately wavelength independent absorption value.[19]

μ_a and μ_s' of these test phantoms (**Figure 2**) were measured by the ISS OxiplexTS™ (ISS Inc., Champaign, Illinois, USA) at 692 nm and 834 nm and the ISS Imagent™ at 760 nm and 831 nm. Both rely on the diffusion approximation [20, 21] assuming a semi-infinite boundary condition,[20] which is fulfilled by these phantoms. For the ISS OxiplexTS™, we applied a multi-distance step-through measurement.[20] A metal holder was fixed firmly on the surface of the phantom with a clamp. The holder contains 3 holes for the detector at defined distances from the source. The emitter is custom-made with 8 optical fibers optimized for the 2 wavelengths, 4 fibers for each wavelength, delivering light to the phantom at one fixed spot (Appendix S1, **Figure A2**). The detector is placed at each of the 3 different distances in three steps, enabling a multi-distance analysis without the need for device calibration. For the ISS Imagent™, we applied the standard adult flexible sensor and followed the standard procedures.

3.3. Absorption Coefficient Offset

IAD is the common standard to analyze spectral optical properties. The conditions in our setup did not completely match the requirements by IAD. IAD assumes a circular beam of light with a radius that the user can specify as a parameter in the analysis. Our setup relies on a rectangular beam, from which we calculated the equivalent radius for IAD. Consequently, wherever the rectangular beam shape guides light closer to the sample border than anticipated by IAD, light loss through side scattering is misinterpreted as increased sample absorption. Furthermore, sample surface imperfections may lead to unaccounted light losses in the IAD analysis. This unaccounted light loss does not affect the general spectral shape of the IAD output but generates a vertical constant offset. The value of this vertical translation is obtained by the mean offset between the values of μ_a with IAD in comparison to ISS OxiplexTS™ at 692 nm and 834 nm.

3.4. Data Analysis

The molar concentrations of the pastes are unknown. We therefore present results as the *volumetric extinction coefficient* ε_v defined by the proportion of dye per unit volume, a variable equivalent to the molar extinction coefficient ε and described by Eq. (3). This idea is in line with Eq. (1), which describes the final μ_a as a sum of individual absorption contributions depending on the chromophores concentrations. The definition of the ε_v – quantity delivers a simple-to-use parameter for recipes that shall guide the production of phantoms with the desired optical properties.

We define the volumetric extinction coefficient ε_v as

$$\varepsilon_v = \frac{1}{\ln(10)} \frac{\mu_a}{P_{\text{color}}}. \quad (3)$$

P_{color} is the proportion in volume of pure color paste (V_{color}) to the total volume of the color paste diluted in silicone SILPURAN® 2420 component A ($V_{\text{component A}}$), described by

$$P_{\text{color}} = \frac{V_{\text{color}}}{V_{\text{color}} + V_{\text{component A}}}. \quad (4)$$

Consequently, ε_v is given in units of mm^{-1} (ml/ml). When fabricating the thin phantoms, dye dilutions were used in the concentrations c_{dye}^j ($j=1,2,3$). This implies the need for a conversion to the pure color paste, namely

$$P_{\text{color}} = c_{\text{dye}}^j \cdot \frac{2\text{g of color}}{200\text{ ml of dye dilution}} \cdot \frac{1}{\rho_{\text{color}}}, \quad (5)$$

where ρ_{color} is the density in grams per milliliter of the pure color paste. Finally, 3 absorption curves (3 different concentrations measured) per color are converted into ε_v using Eq. (3).

These were employed to calculate the standard deviation in ε_v . All spectra were smoothed in the frequency domain by a Butterworth filter (*MATLAB® v. R2014a*, The MathWorks Inc.), with a cutoff frequency $f_c=125\text{ nm}^{-1}$ and a filter order $k=4$. Per color, the ε_v spectra with lowest noise corresponding to the highest concentration c_{dye} was selected for presentation.

3.5. Validation

To validate the design process of optical phantoms with a specific StO_2 , a 600 ml phantom was fabricated. From the same mixture, thin phantoms were manufactured and analyzed with IAD. For this phantom, the target value of total hemoglobin [tHb] was set to 55 μM , which is a common concentration of tHb in the brain of preterm neonates.[4] The normal range of StO_2 for the brain of these infants is 55-85 %.[7] Given the ε_v spectra of the colors, only StO_2 values below approximately 60 % were achievable. The most accurately imitable StO_2 value was estimated to be 38 %, to which our phantom's composition was tailored. The composition of the silicone phantom used for validation is presented in the **Appendix A1, Table A2**. We analyzed the 600 ml phantom with the ISS oximeters using the multi-distance step-through method, described in Section 3.2, for both OxiplexTSTM and ImagentTM.

4. Results

4.1. Volumetric Extinction Coefficients

The ε_v spectra for all evaluated colors are displayed in **Figure 3**.

4.2. Reduced Scattering Coefficients

The μ_s' of the three 600 ml phantoms were determined by the NIRS oximeters. The results of the μ_s' investigated with ISS OxiplexTSTM and ISS ImagentTM are shown in Table 1 together with the values determined for the thin phantoms with the Shimadzu spectrometer and IAD.

4.3. Absorption Coefficient Offset

The constant offset between the IAD and NIRS methods was calculated (according to Sec. 3.3) and the IAD μ_a spectra corrected. This can be seen in **Figure 4**, and the uncorrected spectra are displayed in the inset. The corrected curves agree well with the μ_a measured by the ISS instruments and thus, this seems an adequate way to adjust for the errors in our IAD setup.

4.4 Validation

The ε_v spectra of the studied colors enable the production of phantoms with low oxygenation values. An error minimization problem was solved in MatLab to estimate an absorption

spectrum of biological tissue at 692 nm, 760 nm and 834 nm. To this end, Eq. (2) was solved for the entire spectral range for StO₂ values varying from 25% to 85% using Gaussian weights centered at the wavelengths of interest. The relative residual errors from the designed absorption spectrum were analyzed (Appendix S1, **Figure A3**). With the colors studied in this work, the optimum StO₂ target value was found to be 38 % (target spectrum). The silicone phantom with such intended optical properties was prepared with the colors Red Violet RAL 4002, Helio Green RAL 6004, Green RAL 6010, Black RAL 9011, Dark Red RAL 3000 and White RAL 9010. The target absorption spectrum of a biological tissue with [tHb]=55 μ M and StO₂=38% is shown in **Figure 5**, as well as the designed and measured phantom's absorption spectra. The equivalent values of StO₂ for the wavelengths 692 nm and 834 nm (for OxiplexTSTM), and 760 nm and 831 nm (for ImagentTM) are depicted in **Table 2**. Differences in the target and the designed absorption spectra are expected and arise from the few different dyes available. This applies in particular for the peak in absorption at 760 nm.

5. Discussion

In this paper, we report on optical properties of 11 silicone-soluble color pastes and the fabrication of phantoms mimicking specific oxygen saturations in biological tissue.

The μ_s' calculated by the IAD software increased inversely proportional to the thickness of the sample. Indeed, the rougher the sample's surface, the higher the μ_s' and the lower g . This indicates an additional scattering introduced by the sanded surface of the thin phantoms the influence of which is larger, the thinner the sample layer becomes. To assess this behavior, we evaluated the test phantoms containing the color paste Blue RAL 5022 and White RAL 9010 with ISS OxiplexTSTM and ISS ImagentTM. No inherent scattering was found for this color paste, as displayed in Table 1. This confirms that the measured scattering with IAD of the pure color paste does not originate from the color itself, but from the sanded surface. We observed similar scattering properties for all of the color pastes, except for White RAL 9010.

Consequently, we assumed $\mu_s' = 0.0 \text{ mm}^{-1}$ for all color pastes except White RAL 9010 over the entire measured spectrum.

Between IAD and ISS methods an offset in μ_a was expected. This offset was indeed observed in Sec. 4.3 and can be seen in Fig. 4. The scattering added by surface roughness accounts for this offset in μ_a . Furthermore, with increasing μ_s' , the unaccounted light loss at the sample border increases (as explained in Sec. 3.3), enhancing the offset. If a constant offset is removed, the spectral shape of IAD and ISS methods are in good agreement.

As anticipated, the color paste White RAL 9010 shows no absorption, only scattering features. The remaining colors exhibit absorption peaks in wavelengths shorter than 850 nm. Their spectra monotonically decrease for wavelengths longer than 730 nm, flattening out above 910 nm, where a silicone absorption peak is also present. These characteristics are ideal for the design of optical phantoms in the visible range, providing a rich number of linear combinations available. In the red and near-infrared part of the spectrum, however, only two colors present peaks of absorption: Blue RAL 5022 and Helio Green RAL 6004.

As can be seen in Fig. 5, the absorption slope of the validation phantom corresponds well to the designed spectrum. The designed and measured StO₂ values match (see Table 2) within an error of only 4 %. Deviation from the target and designed StO₂ values are due to the complex shape of the hemoglobin absorption spectrum in the selected wavelengths, which is not possible to mimic completely with the dyes studied.

For designing phantoms with specific spectral features, it is desirable to include further dyes with peaks in the red and near-infrared. Once this is achieved, phantoms mimicking realistic physiological conditions will be produced.

In a clinical setting, phantoms produced with the presented method enable to assess the precision and accuracy of measurement within the error of the designed StO₂. Since the wavelengths of a given oximeter are usually known, in principle, the designed StO₂ can be

calculated for any oximeter. This also implies that as long as the phantom does not implement the hemoglobin spectra completely, this StO₂ value will be different for each oximeter.

6. Conclusions and Prospects

In this study our method for characterizing the optical properties of silicone soluble color pastes was confirmed to be reliable and reproducible. The knowledge of the absorption and scattering properties of these dyes enables to selectively design the optical spectra of silicone phantoms in a specific range. This method is an important step towards the production of long-term stable optical phantoms that mimic biological tissue with specific oxygenation levels. To simulate a broader range of tissue oxygen saturation values the dataset should be expanded with more dyes.

Supporting Information Additional Supporting Information may be found online in the supporting information tab for this article.

Appendix S1, Table A1: Batch numbers of the evaluated color pastes, as provided by *Wacker Chemie AG*, Munich, Germany.

Appendix S1, Table A2: Validation phantom recipe.

Appendix S1, Figure A1: Demonstration of the casting process of thin phantoms.

Appendix S1, Figure A2: Measurement setup for the multi-distance step-through measurement.

Appendix S1, Figure A3: Error minimization problem solved in *MatLab*.

Acknowledgements This work was supported by the Clinical Research Priority Programs (CRPP) Tumor Oxygenation TO₂ and Molecular Imaging Network Zurich MINZ of University of Zurich, the Nano-Tera projects ObeSense, ParaTex and NewbornCare and the Swiss National Science Foundation (project 159490), and the BioEntrepreneur-Fellowship of the University of Zurich, Reference No. BIOEF-17-004. Natasha Tomm, Linda Ahnen and Helene Isler contributed equally to this work.

References

- [1] S. Hyttel-Sorensen, A. Pellicer, T. Alderliesten, T. Austin, F. van Bel, M. Benders, O. Claris, E. Dempsey, A.R. Franz, M. Fumagalli, C. Glud, B. Grevstad, C. Hagmann, P. Lemmers, W. van Oeveren, G. Pichler, A.M. Plomgaard, J. Riera, L. Sanchez, P. Winkel, M. Wolf, and G. Greisen, *BMJ*, **2015**, 350.

- [2] P. Korcek, Z. Stranak, J. Sirc, and G. Naulaers, *J Perinatol*, **2017**, 37.
- [3] F. Scholkmann, S. Kleiser, A.J. Metz, R. Zimmermann, J. Mata Pavia, U. Wolf, and M. Wolf, *Neuroimage*, **2014**, 85 Pt 1.
- [4] Y. Teng, Y. Li, and X. Hou, *International Journal of Mechatronics and Automation*, **2012**, 2.
- [5] P.E. Bickler, J.R. Feiner, and M.D. Rollins, *Anesth Analg*, **2013**, 117.
- [6] S. Hyttel-Sorensen, S. Kleiser, M. Wolf, and G. Greisen, *Biomedical Optics Express*, **2013**, 4.
- [7] S. Kleiser, S. Hyttel-Sorensen, G. Greisen, and M. Wolf, *Comparison of Near-Infrared Oximeters in a Liquid Optical Phantom with Varying Intralipid and Blood Content*, in *Oxygen Transport in Tissue XXXVII*, C.E. Elwell, T.S. Leung, and D.K. Harrison, Editors. Springer, 2016.
- [8] S. Kleiser, N. Nasser, B. Andresen, G. Greisen, and M. Wolf, *Biomedical Optics Express*, **2016**, 7.
- [9] H. Jang, T.J. Pfefer, and Y. Chen, *Optics Letters*, **2015**, 40.
- [10] M. Lindkvist, G. Granåsen, and C. Grönlund, *Spectroscopy Letters*, **2013**, 46.
- [11] J.W. Pickering, C.J. Moes, H. Sterenborg, S.A. Prahl, and M.J. Van Gemert, *Journal of OSA A*, **1992**, 9.
- [12] J.W. Pickering, S.A. Prahl, N. van Wieringen, J.F. Beek, H.J. Sterenborg, and M.J. van Gemert, *Journal of Applied Optics*, **1993**, 32.
- [13] J.G. Symons, E.A. Christie, and M. Peck, *Journal of Applied Optics*, **1982**, 21.
- [14] S.A. Prahl. *Oregon Medical Laser Center, Inverse Adding-Doubling*. [cited 2016; Available from: <http://omlc.org/software/iad/index.html>].
- [15] A.J. Welch and M.J. Van Gemert, *Optical-thermal response of laser-irradiated tissue* Vol. 2. 2011: Springer.
- [16] T. Moffitt, Y.C. Chen, and S.A. Prahl, *Journal of Biomedical Optics*, **2006**, 11.
- [17] H. Isler, C. Germanier, L. Ahnen, J. Jiang, S. Lindner, A. Di Costanzo Mata, T. Karen, S. Sánchez Majos, M. Wolf, and A. Kalyanov, *Journal of Biophotonics*, **2017**.
- [18] S.L. Jacques, *Physics in Medicine and Biology*, **2013**, 58.
- [19] B.W. Pogue and M.S. Patterson, *Journal of Biomedical Optics*, **2006**, 11.
- [20] S. Fantini, M.A. Franceschini, and E. Gratton, *Journal of OSA B*, **1994**, 11.
- [21] J.R. Lorenzo, *Principles of diffuse light propagation: light propagation in tissues with applications in biology and medicine*. 2012: World Scientific.

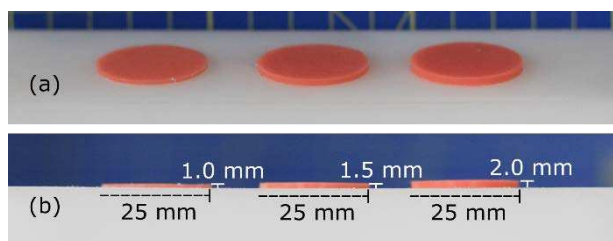


Figure 1. Thin silicone phantoms fabricated in the thicknesses of 1.0 mm, 1.5 mm and 2.0 mm as seen (a) from a side view and (b) from a profile.

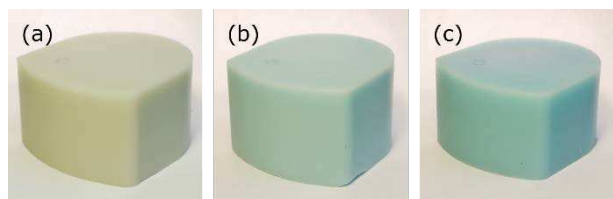


Figure 2. Test phantoms (a) I, with the basic scattering dilution, (b) II, with Blue 5022 added, and (c) III, same as phantom II but with half the amount of White 9010 (Table 1). The phantoms are casted in 600 ml molds and designed to characterize scattering properties of the color pastes.

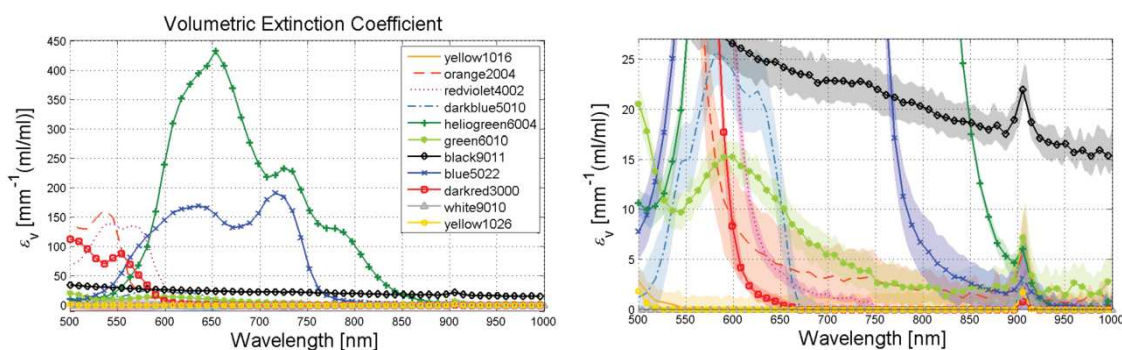


Figure 3. Volumetric extinction coefficient ε_v (1/mm (ml/ml)) of the 11 evaluated colors (left) and enlarged spectra (right). The standard deviation shown for each color is obtained from the evaluation of 3 different concentrations of dye dilution and is too small to be seen in the full range plot (left).

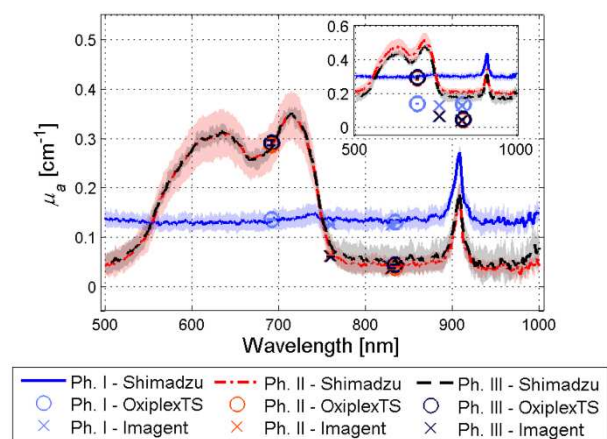


Figure 4. μ_a spectra with their standard deviations of the test phantoms I, II and III corrected by a constant vertical offset. Once this offset is corrected, the spectra of IAD agree well with the μ_a determined with ISS OxiplexTS™ at 692 and 834 nm and ISS Imagent™ at 760 and 831 nm. The inset displays the uncorrected μ_a spectra.

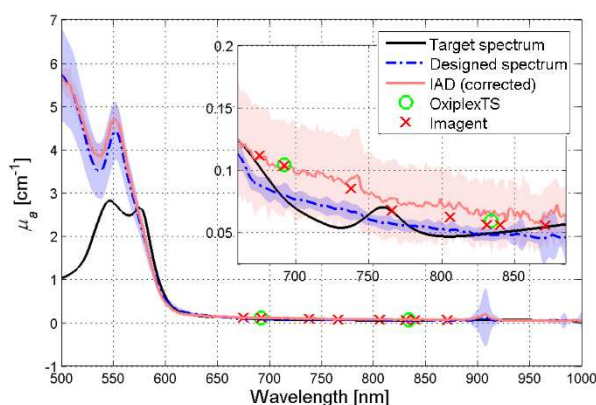


Figure 5. μ_a spectra with their standard deviations of target and designed phantom, as well as measured spectrum evaluated with IAD and corrected as described in Sec. 3.3 and Sec. 4.3. Also shown are the measured μ_a determined with ISS OxiplexTSTM (692 and 834 nm) and a research ISS ImagentTM (675, 692, 738, 766, 806, 831, 840 and 871 nm). These additional wavelengths are illustrated for a better verification of the spectrum. Note that the error bars of the oximeters measurements are too small to be

depicted in the plot.

Table 1. Composition of test phantoms I, II and III (above). Evaluation of median μ_s' and standard deviation with IAD analysis, and mean μ_s' evaluated with ISS OxiplexTSTM and ISS ImagentTM, in units of mm⁻¹. A 5 % error is considered for the oximeters. The wavelengths evaluated are indicated in superscript.

Phantom	I	II	III
V _{White RAL 9010 dye solution}	600 μ l	600 μ l	300 μ l
V _{carbon black}	650 μ l	164 μ l	164 μ l
V _{Blue RAL 5022 dye solution}	0.0 ml	2.5 ml	2.5 ml
$\mu_s'^{692}$	1.06 \pm 0.02	1.02 \pm 0.03	0.52 \pm 0.04
Shimadzu $\mu_s'^{760}$	0.99 \pm 0.02	0.97 \pm 0.04	0.51 \pm 0.05
+ IAD $\mu_s'^{830}$	0.93 \pm 0.03	0.92 \pm 0.03	0.48 \pm 0.05
$\mu_s'^{834}$	0.94 \pm 0.03	0.92 \pm 0.04	0.47 \pm 0.05
ISS OxiplexTS TM $\mu_s'^{692}$	0.94 \pm 0.05	0.97 \pm 0.05	0.46 \pm 0.02
$\mu_s'^{834}$	0.81 \pm 0.04	0.84 \pm 0.04	0.38 \pm 0.02
ISS Imagent TM $\mu_s'^{760}$	0.87 \pm 0.04	0.87 \pm 0.04	0.40 \pm 0.02
$\mu_s'^{830}$	0.79 \pm 0.04	0.78 \pm 0.04	0.33 \pm 0.02

Table 2. StO₂ values of the target spectrum, designed phantom and as observed with ISS OxiplexTSTM (692 and 834 nm) and ISS ImagentTM (766 and 831 nm). The standard deviations in StO₂ of designed phantom arise from a combinatorial analysis of the volumetric extinction coefficients, and the standard deviations from the oximeters from 5 repetitive measurements.

	StO ₂ (%) target	StO ₂ (%) designed	StO ₂ (%) measured
ISS OxiplexTS TM	38.0	34.2 \pm 10.7	30.4 \pm 1.0
ISS Imagent TM	38.0	51.5 \pm 5.8	49.4 \pm 0.3

Graphical Abstract

To validate the correct functioning of near-infrared spectroscopy (NIRS) based oximeters, optical phantoms are necessary. We developed a new approach to create optical phantoms with specific oxygenation values based on combining 11 color pastes for coloring the phantom. We managed to create a phantom that matched the designed oxygenation value within an error of only 4%.



Supporting Information

Characterization of the optical properties of color pastes for the design of optical phantoms mimicking biological tissue

Natasha Tomm^{}, Linda Ahnen, Helene Isler^{*}, Stefan Kleiser, Tanja Karen, Daniel Ostojic, Martin Wolf and Felix Scholkmann*

Table A1 Batch numbers of the evaluated color pastes, as provided by Wacker Chemie AG, Munich Germany.

Color Paste	Batch Number
Yellow RAL 1026	SZ18969
Red Violet RAL 4002	SZ17375
Orange RAL 2004	SZ19077
Yellow RAL 1016	SZ18371
Dark Blue RAL 5010	SZ19848
White RAL 9010	SZ17847
Helio Green RAL 6004	SZ19154
Dark Red RAL 3000	SZ18231
Green RAL 6010	SZ18081
Black RAL 9011	SZ18150
Blue RAL 5022	SZ18480

Table A2 Composition of silicone phantom used for validation. The volume and mass values presented refer to the pure paste. For the fabrication of the phantom, dye dilutions as specified in the Section 3 were used.

Component	Volume	Mass
Silicone comp. A	298.58 ml	316.49 g
Silicone comp. B	300.00 ml	327.00 g
Red Violet RAL 4002	7.66 μ l	8.05 mg
White RAL 9010	661.70 μ l	992.55 mg
Helio Green RAL 6004	0.31 μ l	0.38 mg
Dark Red RAL 3000	669.62 μ l	696.40 mg
Green RAL 6010	59.36 μ l	86.66 mg
Black RAL 9011	20.43 μ l	31.46 mg

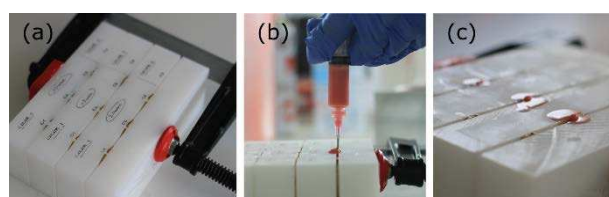


Figure A1. To cast thin phantoms, (a) spacer rings with a small opening are clamped within sanded plastic blocks. Thoroughly mixed and de-aerated silicone is (b) added into the spacer rings and (c) left to cure.

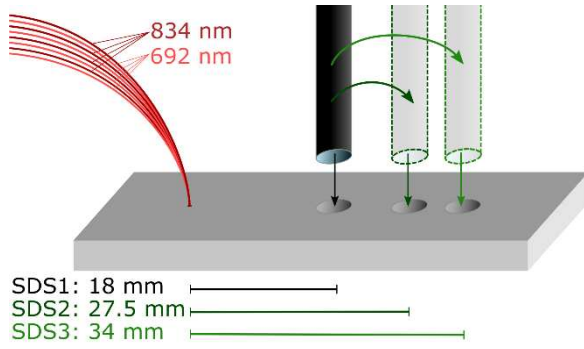


Figure A2. Measurement setup for the multi-distance step-through measurement. There is one detector in use, which is sequentially moved from source detector separation (SDS) 1 to SDS2 and SDS3. 8 light fibers were employed to guide the two wavelengths (692 nm, 834 nm) utilized by OxiplexTSTM.

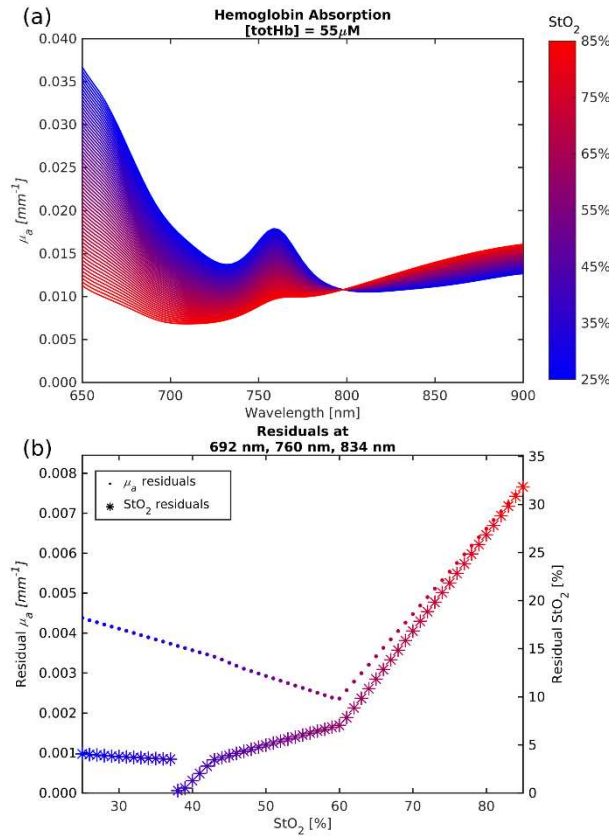


Figure A3. (a) Absorption spectrum of hemoglobin at a concentration of 55 μ M with different values of StO₂, ranging from 25% to 85%. One can notice the change in slope of the curve from negative to positive above 650 nm for a value of StO₂ of approximately 60%. (b) Sum of relative residuals calculated at 692 nm, 760 nm and 834 nm of designed absorption spectra relative to the desired absorption spectra at values of StO₂ between 25% and 85%. Above 60% the residual error increases rapidly up to a point where the designed spectrum of absorption resembles very little the desired spectrum.